

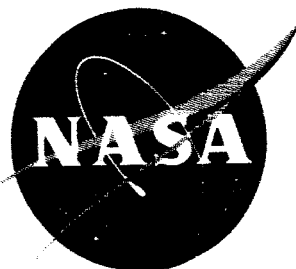
NASA TM X-168

Copy 1

655

NASA TM X-168

X62-71992



TECHNICAL MEMORANDUM

X-168

HIGH-SUBSONIC-SPEED INVESTIGATION OF THE STATIC
LONGITUDINAL AERODYNAMIC CHARACTERISTICS OF
SEVERAL DELTA-WING CONFIGURATIONS FOR
ANGLES OF ATTACK FROM 0° TO 90°

By Bernard Spencer, Jr.

Langley Research Center
Langley Field, Va.

DECLASSIFIED - EFFECTIVE 1-15-64
Authority: Memo Geo. Drobka NASA HQ.
Code ATSS-A Dtd. 3-12-64 Subj: Change
in Security Classification Marking.

GPO PRICE \$

OTS PRICE(S) \$

Hard copy (HC)

Microfiche (MF)

\$2.12
\$0.50

NATIONAL AERONAUTICS AND SPACE ADMINISTRATION
WASHINGTON

December 1959

N65 12694

(ACCESSION NUMBER)

(PAGES)

(NASA CR OR TMX OR AD NUMBER)

(THRU)

(CODE)

(CATEGORY)

X-168

DECLASSIFIED

NATIONAL AERONAUTICS AND SPACE ADMINISTRATION

TECHNICAL MEMORANDUM X-168

HIGH-SUBSONIC-SPEED INVESTIGATION OF THE STATIC

LONGITUDINAL AERODYNAMIC CHARACTERISTICS OF

SEVERAL DELTA-WING CONFIGURATIONS FOR

ANGLES OF ATTACK FROM 0° to 90° *

By Bernard Spencer, Jr.

SUMMARY

12694

An investigation was made in the Langley high-speed 7- by 10-foot tunnel at high subsonic speeds to determine the effect of plan-form geometry on the static longitudinal aerodynamic characteristics of triangular plan-form models at angles of attack from approximately 0° to 90° . The wings had leading-edge sweeps of 55° , 59° , 63° , and 73° . These wings were also tested with folding-type panels located at the wing tip to provide pitch control and increase stability. Variation in plan form of these wing-tip panels included varying the leading-edge sweep from 33.5° to 48° and the ratio of tip-panel area to wing area from 0.20 to 0.40.

All the plan forms had static longitudinal stability with wing-tip extensions retracted, for angles of attack from approximately 25° to 90° but were longitudinally unstable at angles of attack below 25° with the moment center located at the wing centroid of area. Addition of wing-tip panels provided sufficient stability at angles of attack from 0° to approximately 13° for the models having leading-edge sweeps of 59° and 63° . However, pitchup occurred at an angle of attack of approximately 18° at low Mach numbers. The severity of pitchup decreased with increasing Mach number. A model with 73° sweep of the wing leading edge and having tip extensions retained its stability to approximately 23° , which also was the angle of maximum lift. Several geometric modifications to the wing-tip panels including leading-edge flaps, vertical displacement of the tip panels, and leading-edge-sweep variations were unsuccessful in delaying the pitchup noted for the various configurations.

*Title, Unclassified.

DECLASSIFIED - EFFECTIVE 1-13-04
Authority: Memo Geo. Drobka NASA HQ.
Code ATSS-A Dtd. 3-12-64 Subj: Change
in Security Classification Marking




INTRODUCTION

Present interest in vehicles suitable for orbital and space flight has resulted in investigations by the National Aeronautics and Space Administration relative to the aerodynamic characteristics associated with these vehicles. The problems of returning vehicle and man safely from outer space through the earth's atmosphere have caused consideration of numerous vehicles suitable for withstanding excessive heating and aerodynamic and deceleration forces to be encountered by both man and vehicle. Two types of vehicles considered for reentry are the wingless (lifting and nonlifting) vehicles (refs. 1 to 3) and the winged-type vehicle (refs. 4 to 6).

The wingless nonlifting vehicle follows a ballistic path during reentry and utilizes a blunt nose as an aid in reducing the aerodynamic-heating problem. Such vehicles are susceptible to large deceleration loads. The wingless lifting-type vehicle employs low values of lift to control deceleration loads.

Winged-type vehicles may be used for either of two types of reentry maneuver. One type of reentry is accomplished by employing the vehicle as a hypersonic glider flying at normal attitudes and using wing aerodynamic lift to make a skip or very low angle reentry. In the second type of reentry scheme, the vehicle would reenter the atmosphere at an angle of attack approaching 90° thereby providing the high drag type of reentry while maintaining some lift available for the trajectory control required to minimize the aerodynamic heating. This type of vehicle may also enable a pilot-controlled flight and nominal values of lift-drag ratio and thus result in a wider selection of landing points. Folding-type panels which are located at the wing tips and are shielded behind the wing during reentry can be unfolded into the airstream to initiate transition to a glide flight. These panels also provide the vehicle with stability and control during the glide and permit the use of reasonable lift-drag ratios for landing.

In order to provide information with which to evaluate this type of reentry vehicle, the Langley Research Center is currently engaged in a wind-tunnel program covering the subsonic, transonic, and supersonic speed ranges. The present paper presents the results of a wind-tunnel investigation of the static longitudinal aerodynamic characteristics for an angle-of-attack range from 0° to 90° and at Mach numbers from 0.4 to 0.90 of various wing and folding-type-panel combinations considered suitable for reentry into the earth's atmosphere.



SYMBOLS

The data presented in this paper are referenced to the stability axis system. (See fig. 1.) The moment center location for each of the configurations tested was at the wing-alone centroid of area which corresponds to the theoretical wing center-of-pressure location at hypersonic speeds with the vehicle at an angle of attack of 90° . (See fig. 2.) The symbols used in this investigation are defined as follows:

| | |
|------------------|---|
| C_L | lift coefficient, $\frac{\text{Lift}}{qS_w}$ |
| C_D | drag coefficient, $\frac{\text{Drag}}{qS_w}$ |
| C_m | pitching-moment coefficient, $\frac{\text{Pitching moment}}{qS_w \bar{c}_w}$ |
| $\Delta C_{L,t}$ | incremental lift provided to configuration by addition of wing-tip panels, $(C_L)_{\text{panels on}} - (C_L)_{\text{panels off}}$ |
| q | dynamic pressure, lb/sq ft |
| α | angle of attack, deg |
| A | aspect ratio of wing, wing-tip panels off, $\frac{b_w^2}{S_w}$ |
| S_w | area of wing, wing-tip panels off, sq ft |
| S_t | area of wing-tip panel, sq ft |
| b_w | span of wing, wing-tip panels off, ft |
| \bar{c}_w | mean aerodynamic chord of wing, wing-tip panels off, ft |
| δ_n | wing-tip panel leading-edge flap deflections (positive for flap leading edge up), deg |
| Λ_{le} | leading-edge sweep of wing or wing-tip panels, depending on subscript, deg |
| M | Mach number |
| x, y, z | coordinates |

Subscripts:

| | |
|---|----------------------------------|
| w | wing |
| t | wing-tip panel |
| n | wing-tip-panel leading-edge flap |

MODEL DESCRIPTION

Drawings of the various models tested are presented as figure 2 and the geometric characteristics of the wings are summarized in table I. A photograph of one of the models shown mounted in the Langley high-speed 7- by 10-foot tunnel is given in figure 3.

The wings used in this investigation consisted of flat-plate sections with rounded leading edges and beveled trailing edges. Variations in the wing plan forms consisted of variations in the leading-edge sweeps of 55° , 59° , 63° , and 73° while the spans and areas were held constant for the 55° , 59° , and 63° wings. The 73° sweptback wing had the same span as the other wings, but had a larger plan-form area. (See table I.) The wing-tip panels consisted of flat-plate sections with rounded leading edges and beveled trailing edges and had variations in leading-edge sweeps of 33.5° , 40° , and 48° , and in plan-form area from 0.20 to 0.40 of the total wing area.

The vertical fins were located outboard of the wing-tip panel and were flat-plate sections. The geometric characteristics of the fuselages are given in figure 2. The ogive sections of the fuselages were approximately 36 percent of the fuselage length on the 55° , 59° , and 63° sweptback wings and approximately 62 percent of the fuselage length on the 73° sweptback wing. Leading-edge flaps were used on the wing-tip panels having a leading-edge sweep of 33.5° and a ratio of tip-extension area to wing area of 0.32. These flaps were approximately $0.70b/2$ of the tip-extension span in length and were pivoted at approximately 10 percent of the tip-extension mean aerodynamic chord. At 0° deflection the leading edge of the flap coincided with the leading edge of the wing-tip panel.

TESTS AND CORRECTIONS

Tests were made in the Langley high-speed 7- by 10-foot tunnel for a Mach number range from 0.40 to 0.90 corresponding to a Reynolds number range of approximately 2.66×10^6 to 3.89×10^6 based on the wing-alone mean aerodynamic chord. The apparatus employed for attaining an

DECLASSIFIED

5

angle-of-attack range from -2° to 93° consisted of an adapter suitable for sting mounting and a quadrant with holes set approximately 22° apart. The location of these holes enabled initial settings of 12° , 34° , 56° , and 78° to be preset manually on the adapter, intermediate angles being attainable by means of the tunnel angle drive system.

An angle-of-attack range from -2° to 93° was obtained for Mach numbers from 0.40 to 0.80 but was limited to approximately -2° to 47° at a Mach number of 0.90 because of the load limits of the balance. Jet-boundary corrections determined by the methods of reference 7 and block-age corrections determined by the methods of reference 8 were found to be negligible for these tests and therefore were not applied to the data. The angle of attack has been corrected for deflection of the sting support system and balance under load.

RESULTS AND DISCUSSION

The effects of wing sweep on the tail-off configuration are presented in figure 4(a) for Mach numbers of 0.60, 0.80, and 0.90. An unstable variation of pitching-moment curve up to maximum lift is noted for the three configurations as would be expected for the moment-center location used. This location, the centroid of area of the wing, was considered to be reasonable since it should minimize the trim forces required in the 90° attitude. Stable variation of pitching-moment curve above maximum lift is noted, however, because of a negative lift-curve slope and because the center of pressure is forward of the moment center for the three wings. The effect of increasing Mach number had little or no effects on decreasing the degree of longitudinal instability for all three wings.

The addition of wing-tip panels to the three wings (fig. 4(b)) provided longitudinal stability for the 63° and 59° sweptback wings up to an angle of attack of approximately 13° but did not make the 55° swept-back wing stable, probably because of the relatively short moment arm of the panels.

The effect of increasing the sweep of the wing-tip panels (fig. 5) indicates small changes in tail-on lift-curve slope and stability at a Mach number of 0.60. Increasing the Mach number, however, indicates definite increases in stability with increasing tip-panel sweep and large reductions in the degree of pitchup associated with all three tip panels at a Mach number of 0.60.

0371301030

Increasing the ratio of wing-tip panel area to wing-area indicates large changes in lift-curve slope and stability due to increased effective configuration aspect ratio. (See fig. 6.) The effectiveness of the wing-tip panels in providing stability is seen to decrease rapidly for the three panel sizes tested at Mach number of 0.60 above an angle of attack of approximately 18° . The degree of pitchup is reduced markedly by increasing Mach number.

The loss of wing-tip-panel effectiveness indicates possible tip-panel stalling. Attempts were made to alleviate the tip-panel stall by deflecting the wing-tip-panel leading edge down to decrease the local angle of attack and by displacing the tip panels vertically up. The effects of these modifications on the 63° sweptback wing with the 33.5° sweptback wing-tip panel are presented as figure 7. The effect of deflecting the wing-tip-panel leading edge is seen to be slight in that pitchup occurs at approximately the same angle of attack as for the undeflected configuration. Displacing the wing-tip panel vertically results in an increase in stability at low angles of attack throughout the Mach number range and also reductions in lift-curve slope up to $C_{L_{max}}$ but produced no improvement in the pitchup characteristics.

Various modifications were employed in an attempt to decrease the pitchup tendencies associated with the selected configurations tested. These modifications included employing 55° sweptback wing with a 48° sweptback wing-tip panel and using a 73° sweptback wing with a 48° sweptback wing-tip panel. (See fig. 8.) The 73° wing indicates a stable, linear variation of pitching moment with angle of attack to the maximum angle attainable at a Mach number of 0.60. For this reason this configuration was tested at a lower Mach number of 0.40 in order to obtain the aerodynamic characteristics of this configuration at higher angles of attack. From figure 8(b) this configuration is seen to possess desirable stability characteristics up to an angle of attack of approximately 23° , corresponding to the angle for maximum lift.

A comparison of the aerodynamic characteristics of the configurations with the 55° and 63° sweptback wings presented in figure 8 simulating reentry, transition from reentry to glide, and glide-flight conditions are presented in figure 9. When glide-flight conditions were simulated, the wing-tip panels were set at a dihedral angle of 0° . For reentry simulation, the wing-tip-panel dihedral angle was 90° , which represents a folded panel shielded from heating. The transition phase was simulated with a wing-tip-panel dihedral angle of 45° . From figure 9 both configurations are seen to possess adequate stability for Mach numbers of 0.60 and 0.80 in simulated transition and reentry attitudes. In order for these configurations to be viewed as desirable reentry configurations, however, more desirable glide conditions should be obtained by modifications of the existing configurations.

In order to show the variation with angle of attack of the lift associated with the wing-tip panels, figure 10 has been prepared. In this figure the increments between panel-on and panel-off lift coefficients are presented through an angle-of-attack range from 0° to approximately 40° and at a Mach number of 0.60 for the various configurations tested. Also presented for comparison purposes are the wing-alone lift coefficients. It must be remembered that the actual loads on the wing-tip panels were not isolated and that the increments presented include the increases in lift on the wing associated with the increased aspect ratio of the configuration.

Figure 10(a) presents the effect of wing sweep on the lift increments associated with the wing-tip panels. The results indicate that, as the wing sweep is reduced, the maximum lift contributed by the wing-tip panels decreases. Comparison with the wing-alone lifts shows that, although the wing-tip panels increase the area by only 30 percent, the rather large increase in aspect ratio makes possible lift increments equal to, or greater than, the wing-alone lift for angles of attack up to about 10° . However, a rather severe reduction in the rate of change of the incremental lifts occurs above about 10° and is responsible for the undesirable pitchup characteristics already noted in connection with figure 4(b).

The effect of the sweep angle of the wing-tip panels is shown in figure 10(b) and it will be observed that the lift associated with these panels is relatively insensitive to sweep for the range of sweep angles investigated. However, as would be expected, there is an appreciable effect of panel size as indicated in figure 10(c).

The effect of attaching the wing-tip panels on fins above the wing-chord plane and the effect of vertical-tail end plates can be seen in figure 10(d). The end-plate effect increases the lift above an angle of attack of about 10° whereas the effect of attaching the wing-tip panels above the wing plane on vertical fins was negligible.

CONCLUSIONS

An investigation was made in the Langley high-speed 7- by 10-foot tunnel at Mach numbers from 0.60 to 0.90 to determine the effects of plan-form geometry on the static longitudinal aerodynamic characteristics of triangular plan-form models at angles of attack from approximately 0° to 90° . The moment center for all models was at the centroid of area of the basic wings. The results of the investigation lead to the following conclusions:

SECRET

03710201030
[REDACTED]

1. All the basic-wing configurations had static longitudinal stability at angles of attack from about 25° to 90° but were longitudinally unstable at angles of attack below 25° .

2. Addition of wing-tip extensions made the models with leading-edge sweep of 59° and 63° longitudinally stable at angles of attack from 0° to about 13° . However, pitchup occurred at an angle of attack of about 18° at low Mach numbers. The severity of pitchup decreased as the Mach number was increased. A model with 73° sweep of the wing leading edge and having tip extensions retained its stability to an angle of attack of about 23° , which was also the angle of attack for maximum lift.

3. Several geometric modifications to the wing-tip extension including use of a nose flap, vertical displacement of the tip extension, and various sweeps of the tip extension were unsuccessful in delaying pitchup of the various configurations.

Langley Research Center,
National Aeronautics and Space Administration,
Langley Field, Va., August 17, 1959.

[REDACTED]

REF ID: A58070

REFERENCES

1. Faget, Maxime A., Garland, Benjamine J., and Buglia, James J.: Preliminary Studies of Manned-Satellites - Wingless Configuration: Nonlifting. NACA RM L58E07a, 1958.
2. Bird, John D., and Reese, David E., Jr.: Stability of Ballistic Reentry Bodies. NACA RM L58E02a, 1958.
3. Allen, H. Julian, and Eggers, A. J., Jr.: A Study of the Motion and Aerodynamic Heating of Ballistic Missiles Entering the Earth's Atmosphere at High Supersonic Speeds. NACA Rep. 1381, 1958. (Supersedes NACA TN 4047.)
4. Rainey, Robert W.: Static Stability and Control of Hypersonic Gliders. NACA RM L58E12a, 1958.
5. Penland, Jim A., and Armstrong, William O.: Preliminary Aerodynamic Data Pertinent to Manned Satellite Reentry Configurations. NACA RM L58E13a, 1958.
6. Paulson, John W.: Low-Speed Static Stability Characteristics of Two Configurations Suitable for Lifting Reentry From Satellite Orbit. NASA MEMO 10-22-58L, 1958.
7. Gillis, Clarence L., Polhamus, Edward C., and Gray, Joseph L., Jr.: Charts for Determining Jet-Boundary Corrections for Complete Models in 7- by 10-Foot Closed Rectangular Wind Tunnels. NACA WR L-123, 1945. (Formerly NACA ARR L5G31.)
8. Herriot, John G.: Blockage Corrections for Three-Dimensional-Flow Closed-Throat Wind Tunnels, With Consideration of the Effect of Compressibility. NACA Rep. 995, 1950. (Supersedes NACA RM A7B28.)

0371028 1030

TABLE I.- GEOMETRIC CHARACTERISTICS OF WINGS

Body:

| | |
|---|-------|
| Maximum diameter, in. | 2.13 |
| Length used on wings with sweep of 63°, 59°, and 55°, in. | 11.00 |
| Length used on wing with 73° sweep, in. | 18.35 |
| Base area, sq in. | 3.18 |

63° sweptback wing:

| | |
|---|-------|
| Span, in. | 8.25 |
| Root chord, actual, in. | 11.0 |
| Tip chord, in. | 3.3 |
| Area, sq ft | 0.409 |
| Mean aerodynamic chord, in. | 7.85 |
| Center of moment area from wing apex, in. | 7.08 |
| Aspect ratio | 1.15 |

59° sweptback wing:

| | |
|---|-------|
| Span, in. | 8.25 |
| Root chord, actual, in. | 11.00 |
| Tip chord, in. | 3.30 |
| Area, sq ft | 0.409 |
| Mean aerodynamic chord, in. | 7.85 |
| Center of moment area from wing apex, in. | 6.67 |
| Aspect ratio | 1.15 |

55° sweptback wing:

| | |
|---|-------|
| Span, in. | 8.25 |
| Root chord, in. | 11.00 |
| Tip chord, in. | 3.3 |
| Mean aerodynamic chord, in. | 7.85 |
| Area, sq ft | 0.409 |
| Center of moment area from wing apex, in. | 6.34 |
| Aspect ratio | 1.15 |

73° sweptback wing:

| | |
|--|-------|
| Span, in. | 8.25 |
| Root chord, in. | 18.35 |
| Tip chord, in. | 5.50 |
| Mean aerodynamic chord, in. | 13.06 |
| Area, sq ft | 0.684 |
| Center of moment area from wing apex | 11.81 |
| Aspect ratio | 0.693 |

L
5
4
8

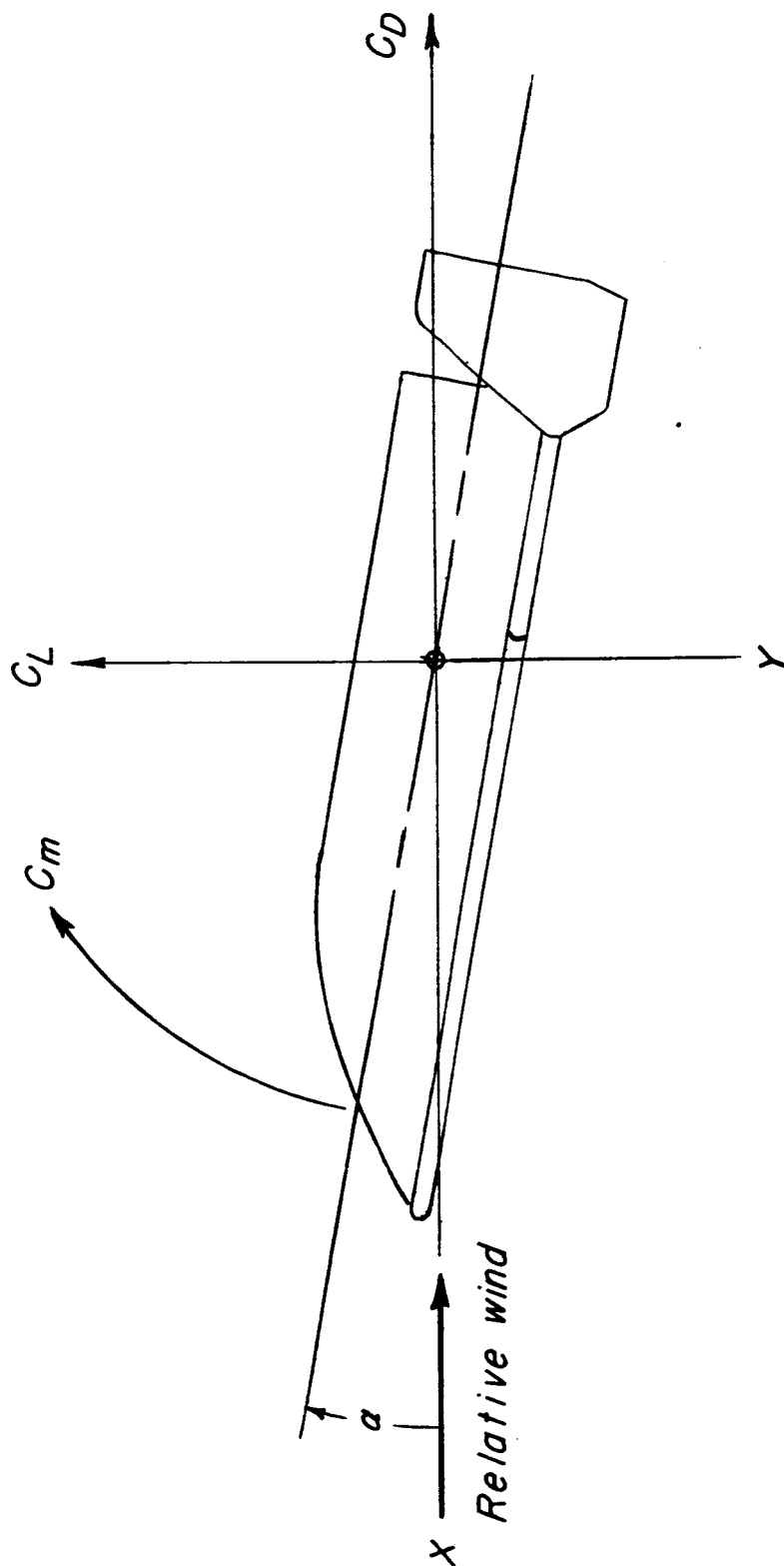
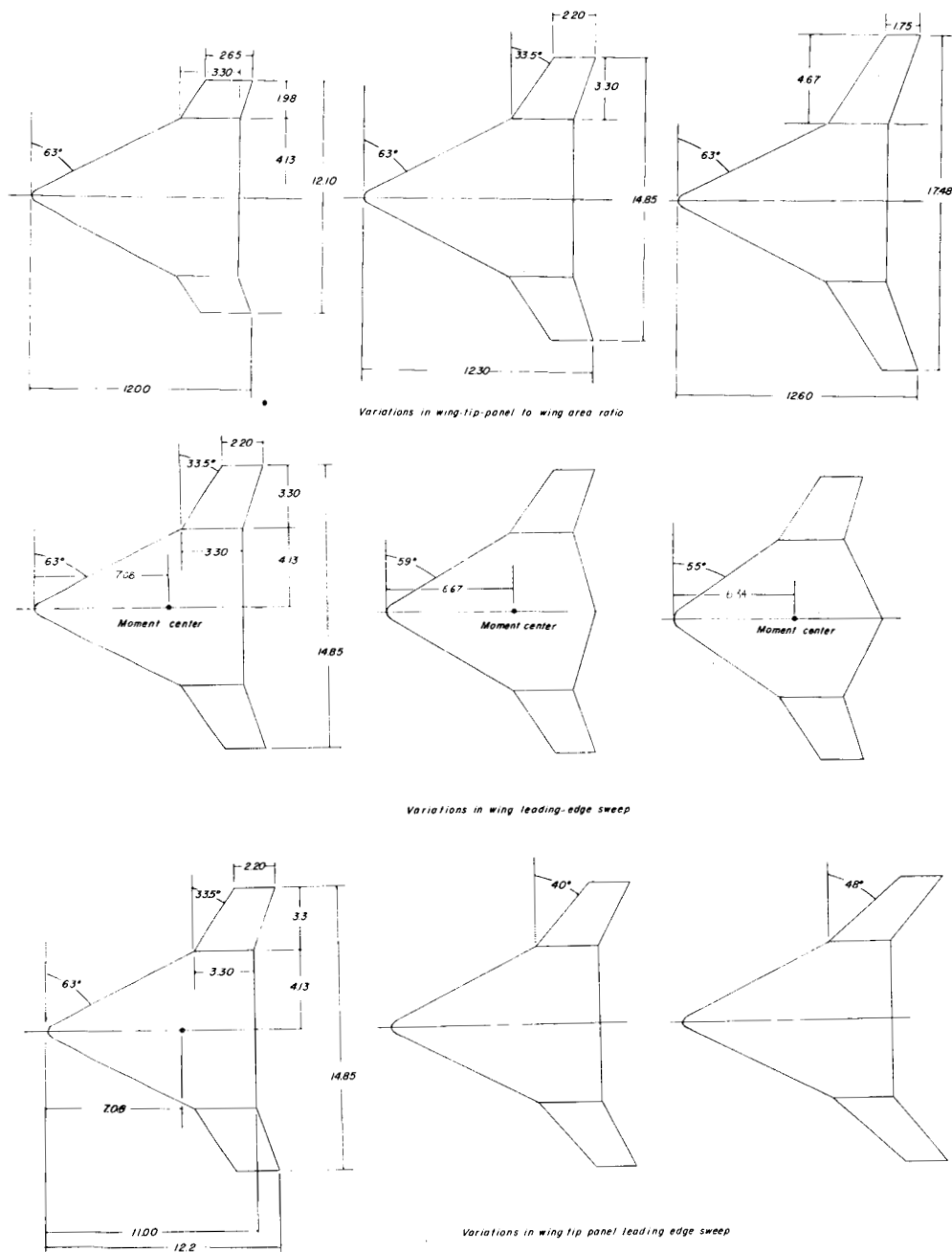
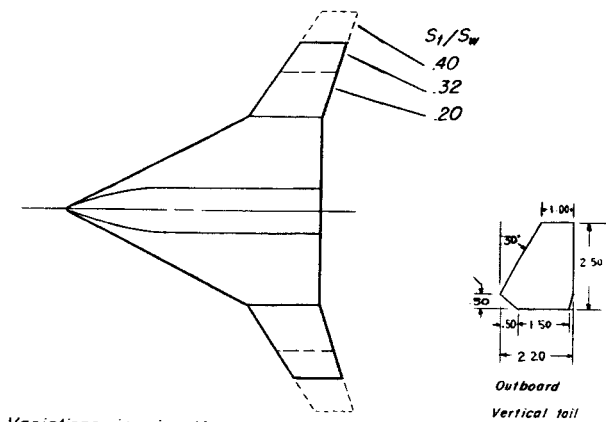


Figure 1.- Stability-axis system with arrows indicating the positive directions of forces, moments, and angular deflections.

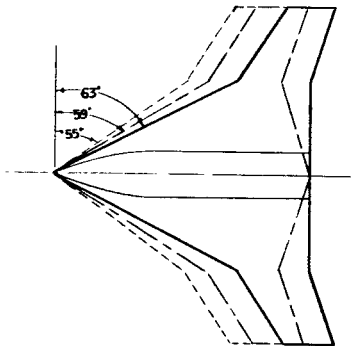


(a) Details of plan forms.

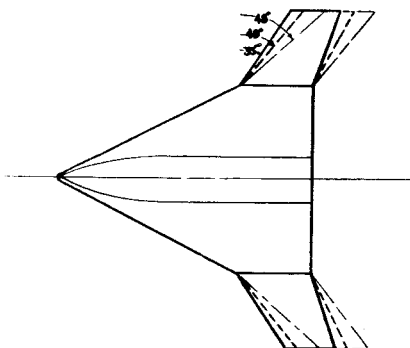
Figure 2.- Geometric characteristics of the plan forms including variations in sweeps and relative wing-tip-panel sizes. All linear dimensions are in inches.



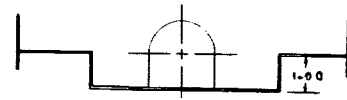
Variations in wing-tip-panel to wing area ratio



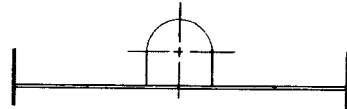
Variation in wing leading-edge sweep



Variations in wing-tip-panel leading-edge sweep

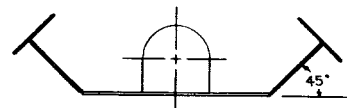


Displaced wing-tip panel

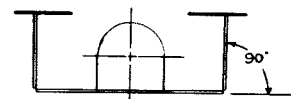


Wing-tip panel in normal position

Configuration glide condition



Configuration transition condition

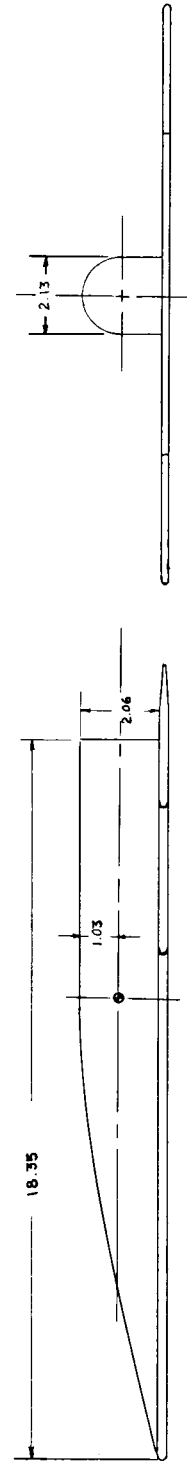
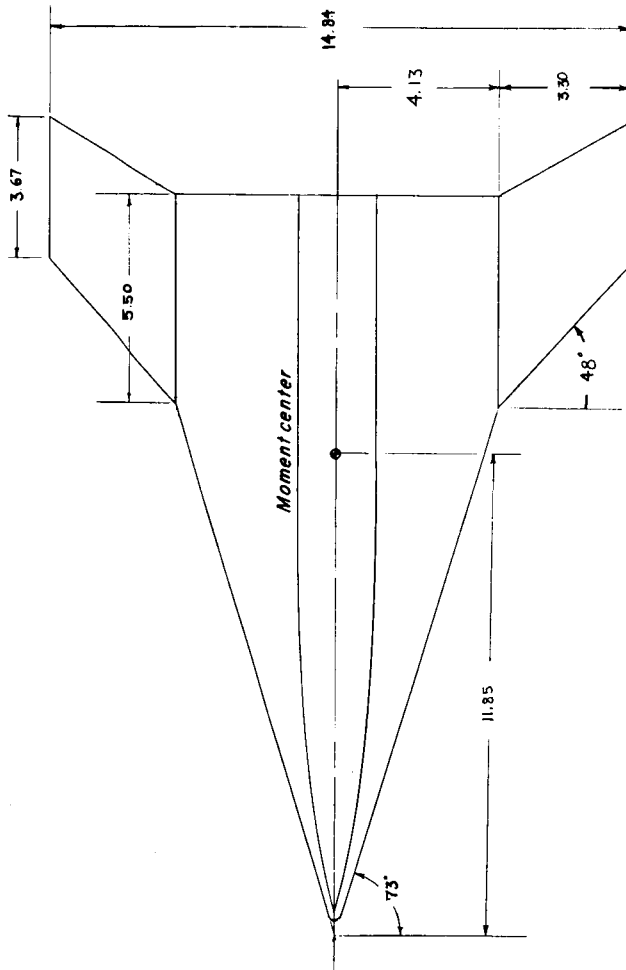


Configuration reentry condition

(b) Superposition of plan-form variations and wing-tip-panel position in simulating reentry, transition, and glide-flight conditions.

Figure 2.- Continued.

03791200 1730

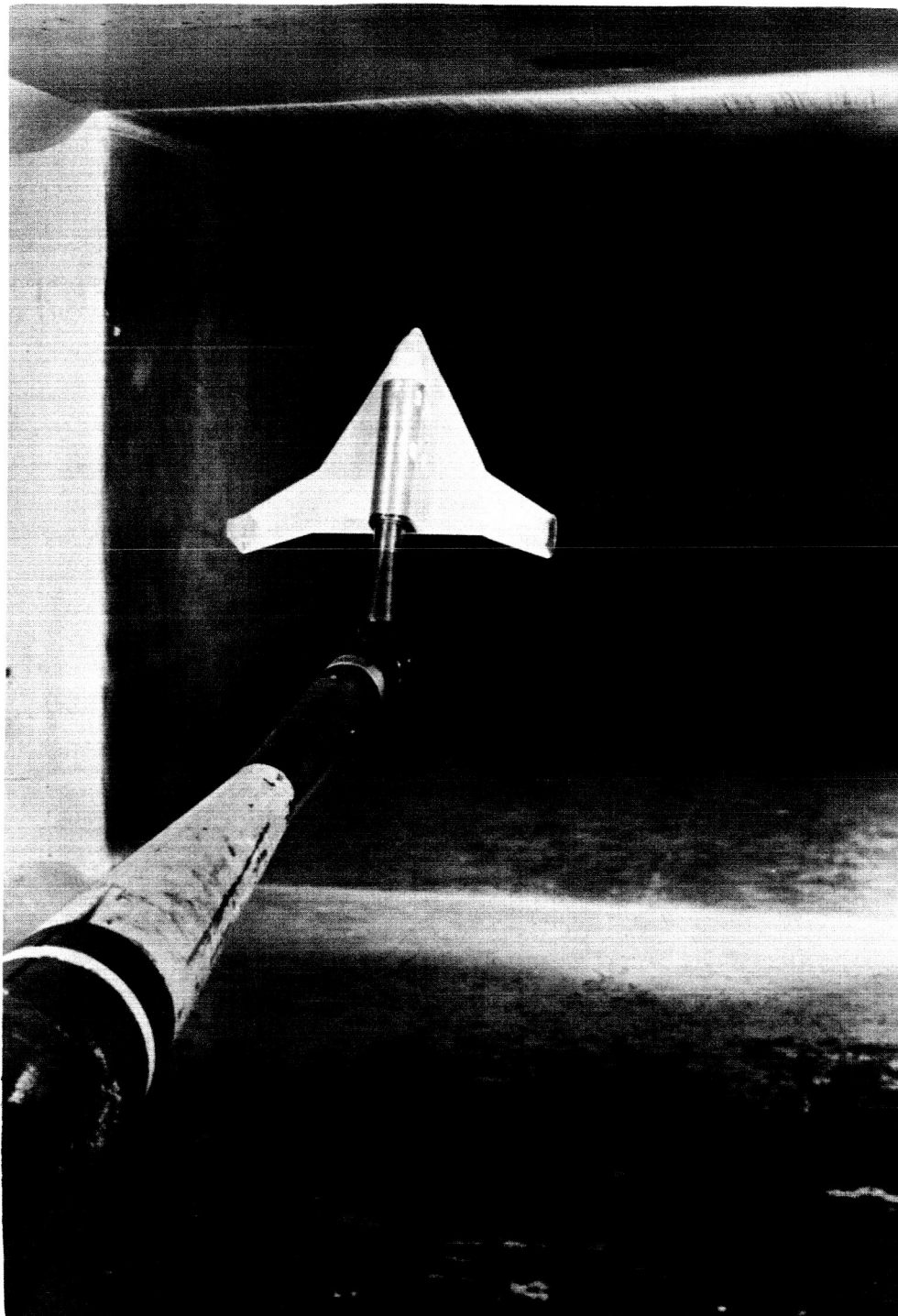


(c) Details of 73° sweptback wing with wing-tip panel swept back 48° .

Figure 2.- Concluded.

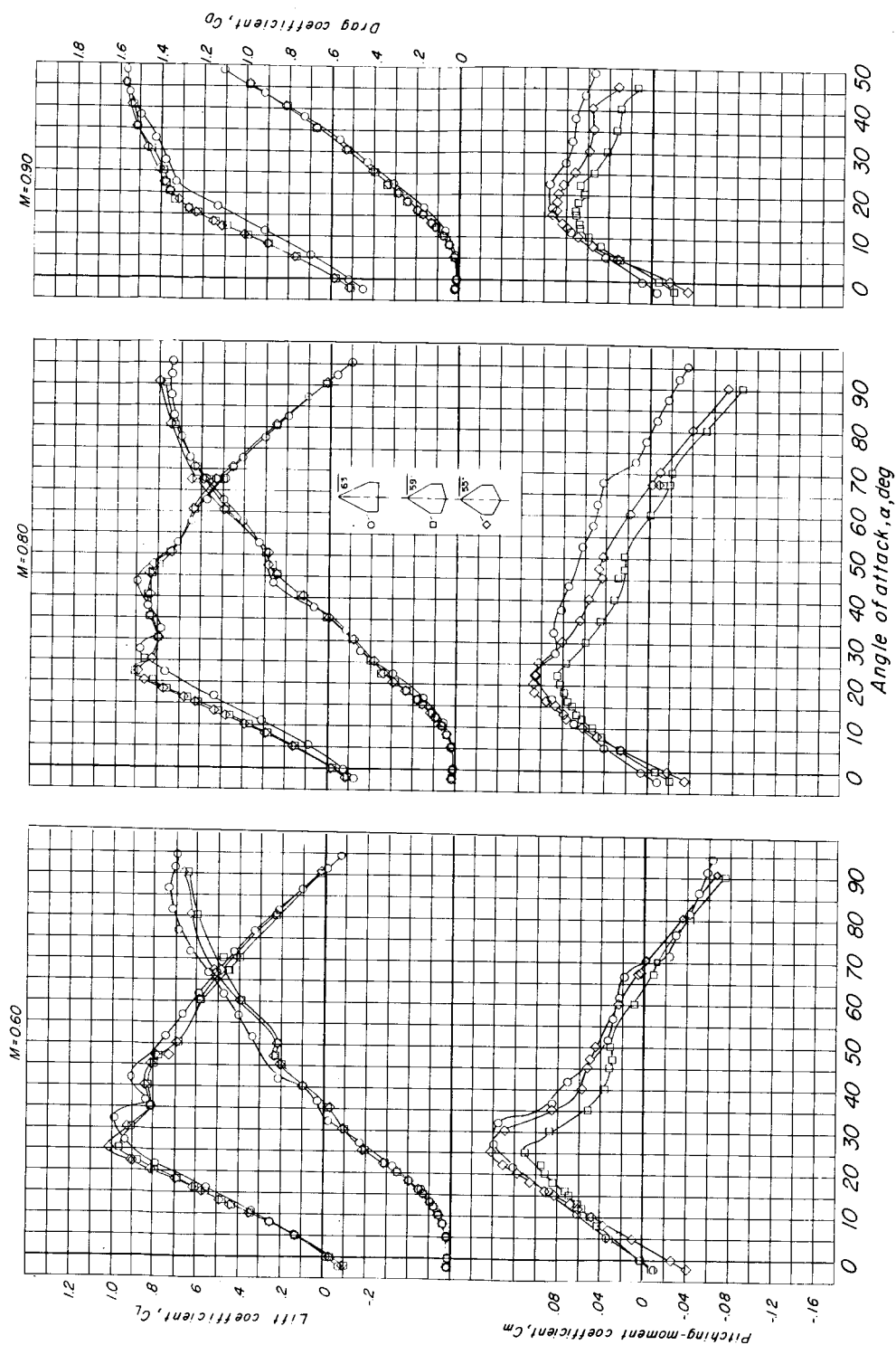
DECLASSIFIED

15



L-58-3497

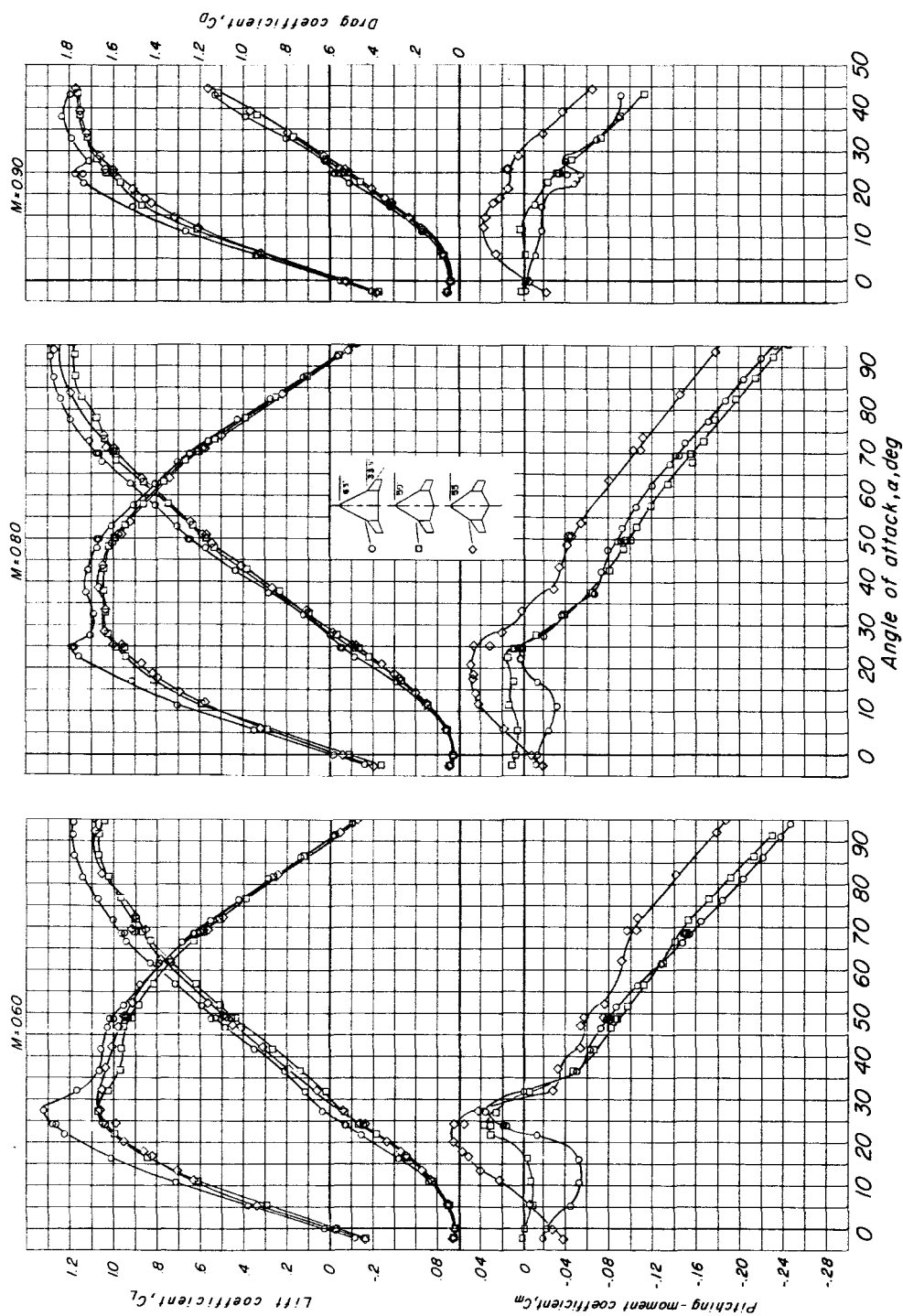
Figure 3.- Photograph of one of the models mounted in the Langley high-speed 7- by 10-foot tunnel.



(a) Wing-tip panels off.

Figure 4.- The effects of wing sweep on the variation of aerodynamic characteristics with angle of attack.

DECLASSIFIED



(b) Wing-tip panels and vertical tails on. $St/S_w = 0.32$; $\Lambda_{te,t} = 33.5^\circ$.

Figure 4. - Concluded.

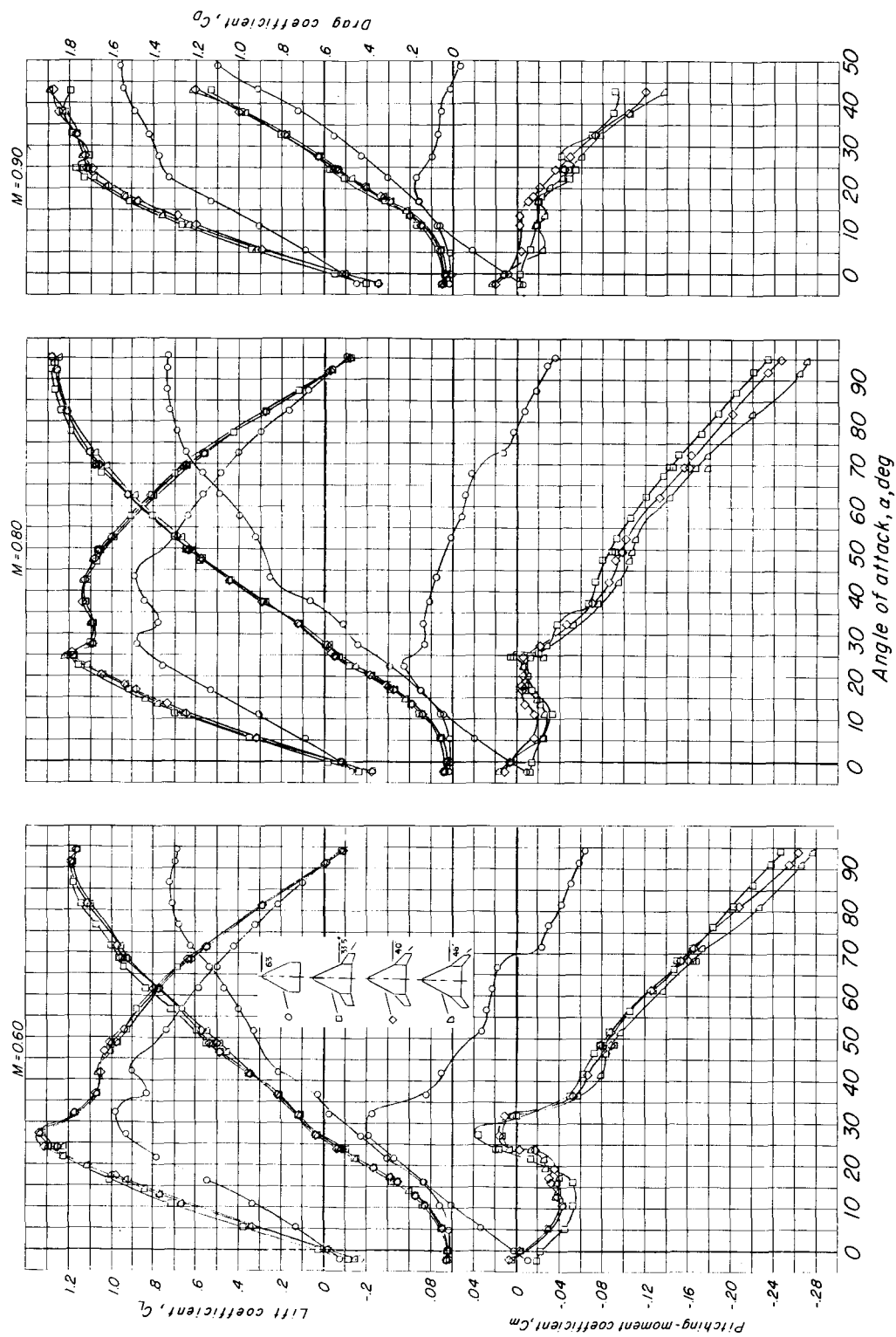


Figure 5.- The effects of wing-tip-panel sweep on the variation of aerodynamic characteristics with angle of attack for the configuration having a 63° sweptback wing. Vertical tails on; $St/S_w = 0.32$.

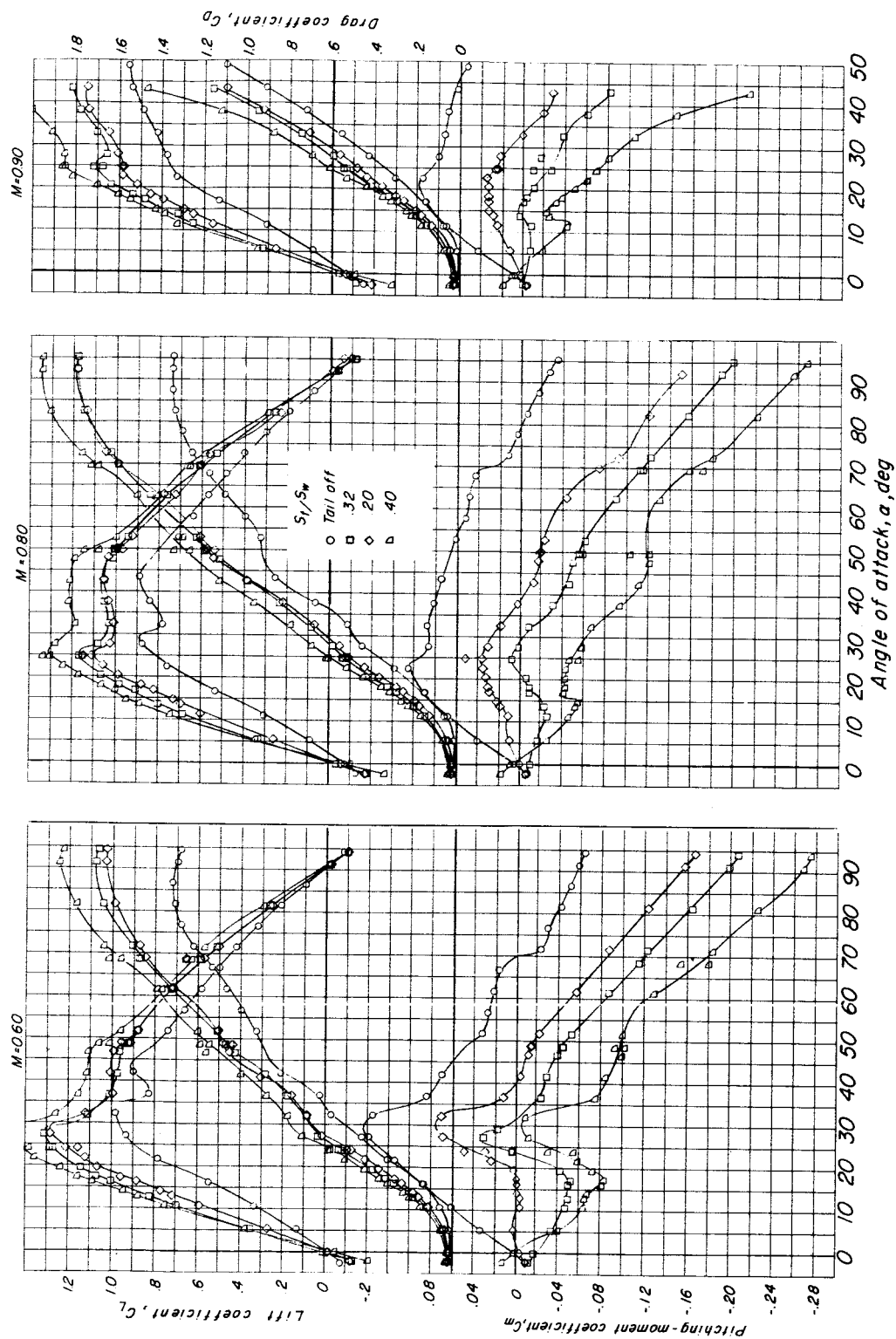


Figure 6.- The effects of wing-tip-panel size on the variation of aerodynamic characteristics with angle of attack for the configuration having a 630 sweptback wing. Vertical tails off; $A/c, t = 33.5^\circ$.

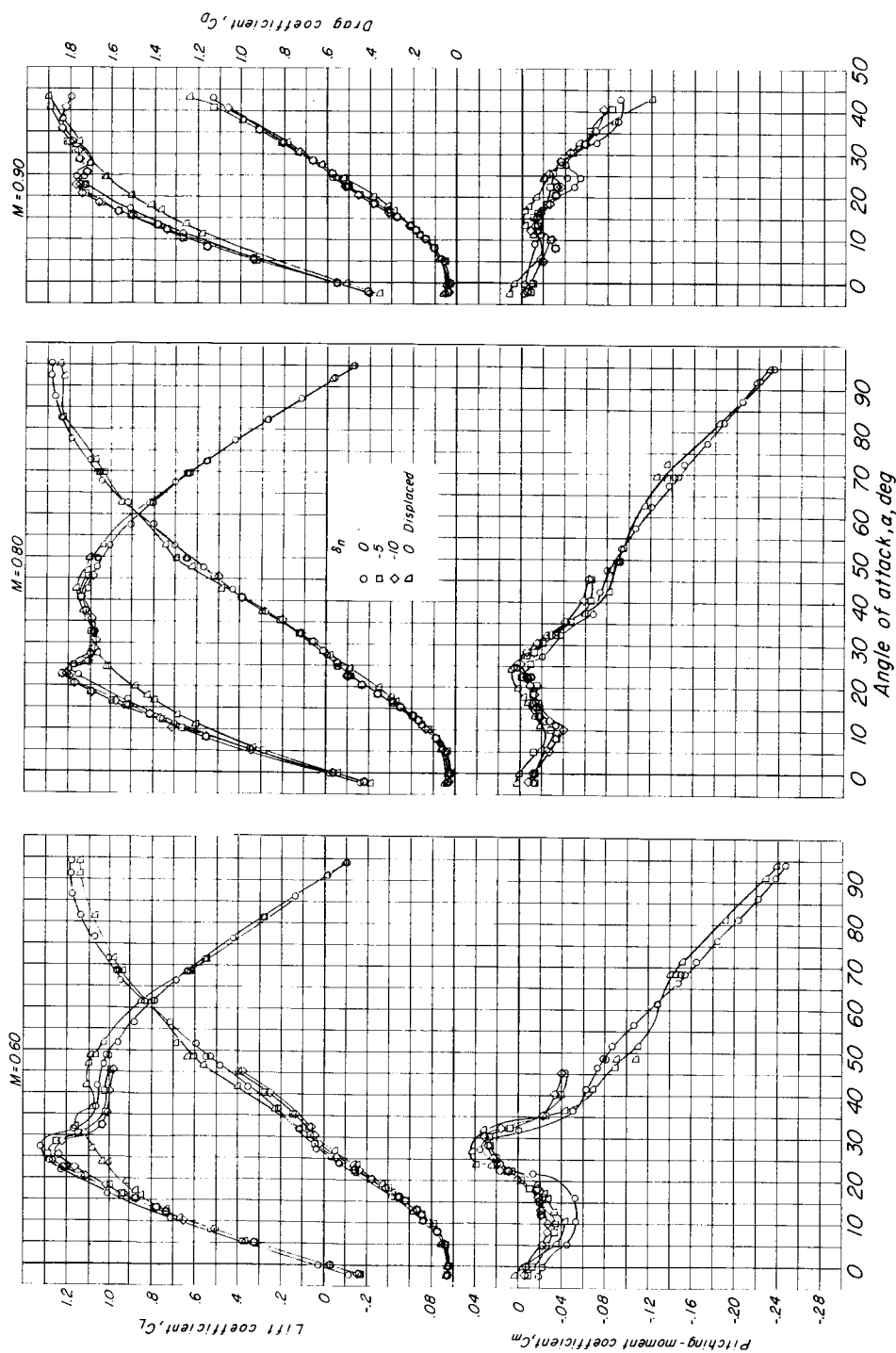


Figure 7.- The effect of wing-tip-panel height and leading-edge flap deflection on the variation of aerodynamic characteristics with angle of attack for the configuration having a 63° sweptback wing, 33.5° sweptback wing-tip panel, and $St/S_w = 0.32$. Vertical tails on.

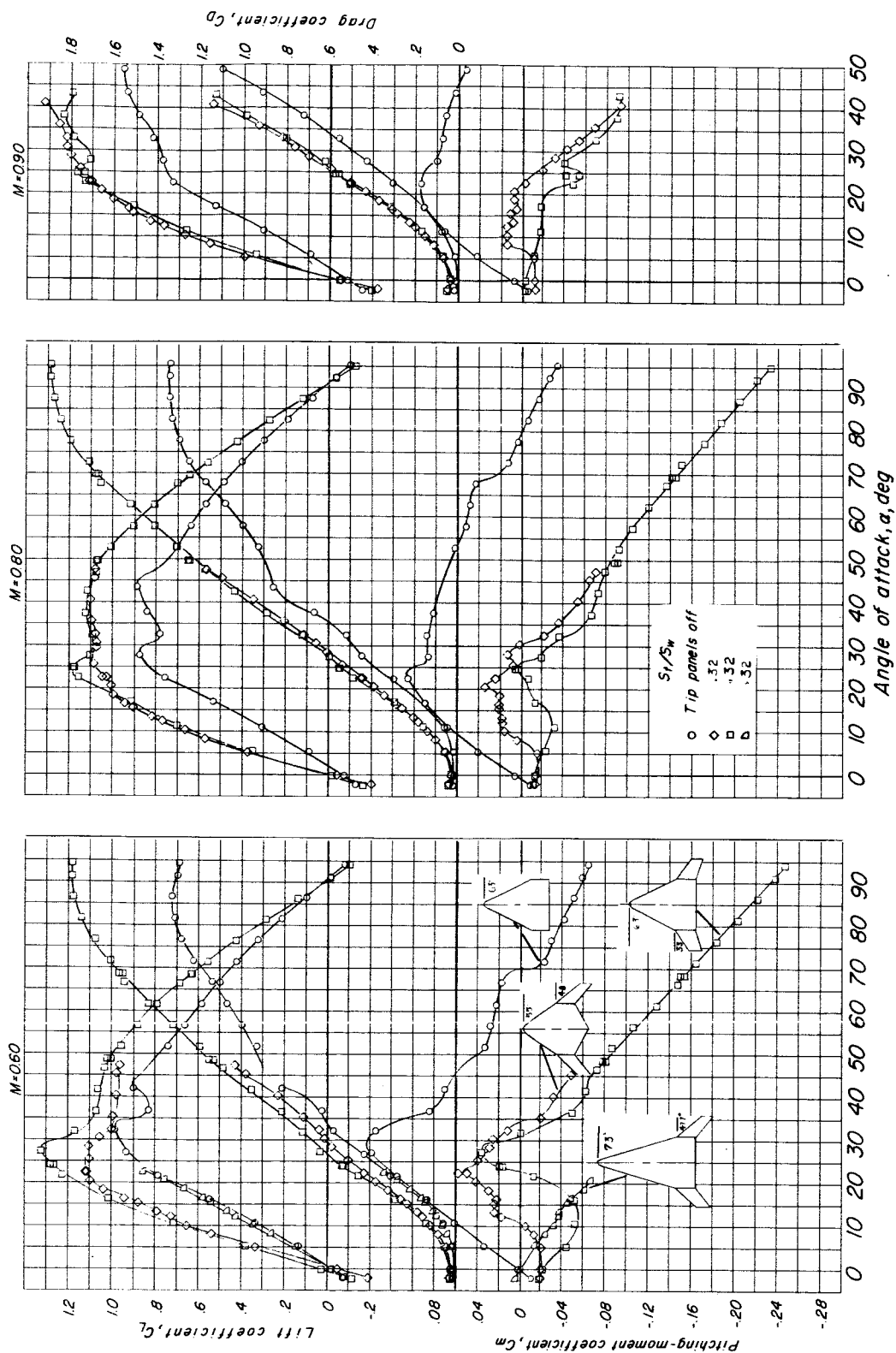


Figure 8.- The effects of various combined modifications on the variation of aerodynamic characteristics with angle of attack.

0317221030

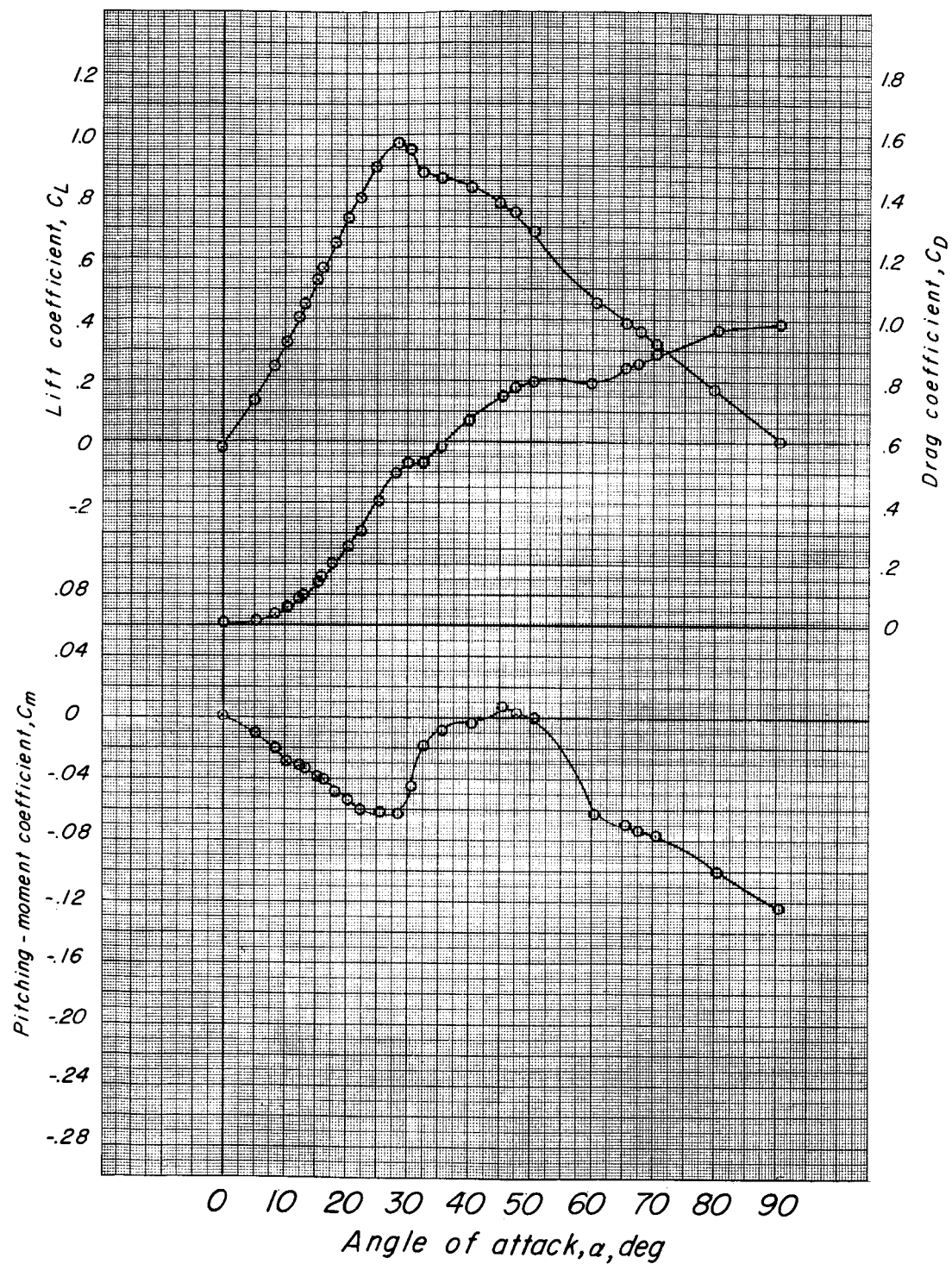


Figure 8.- Concluded.

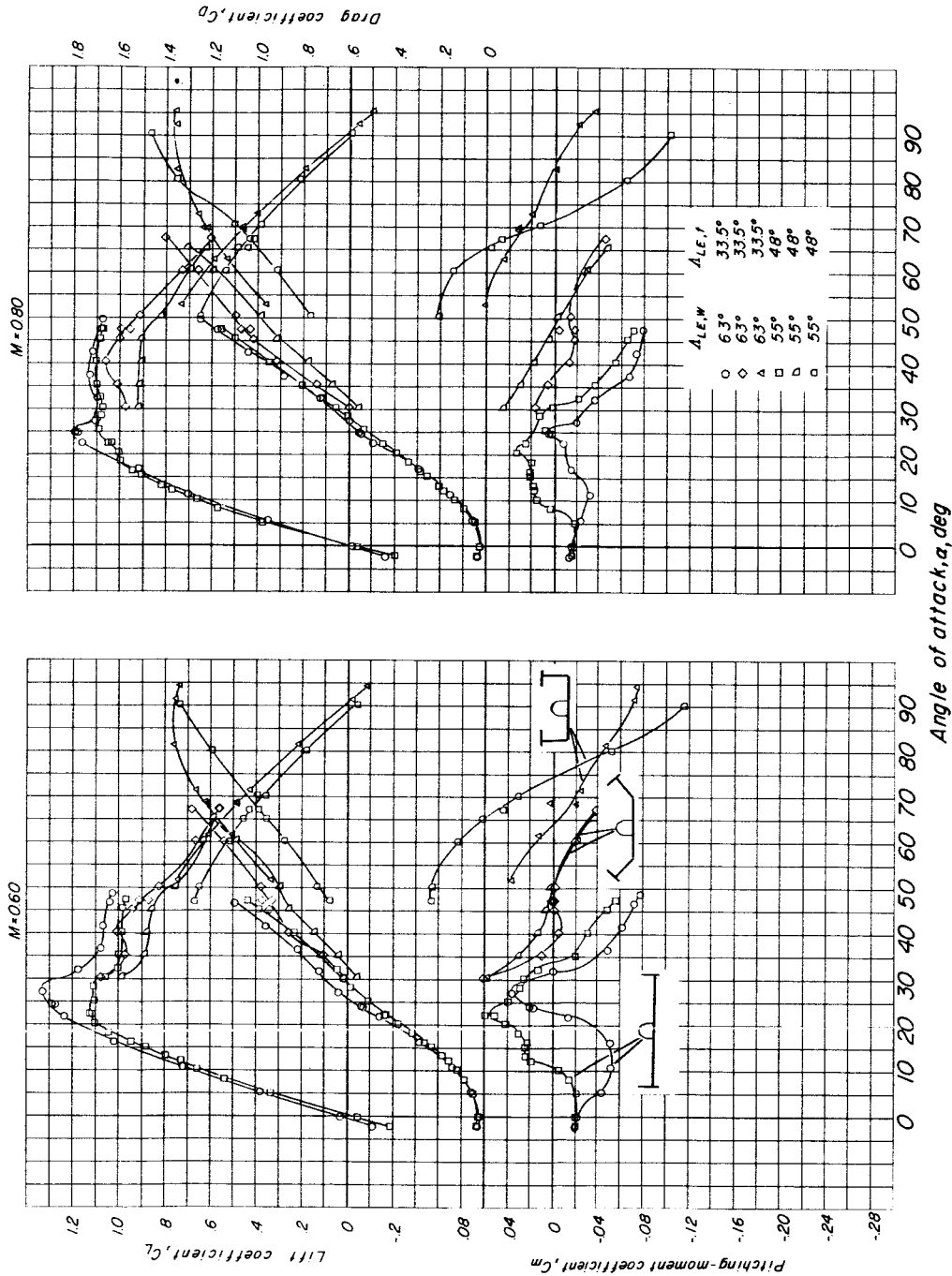
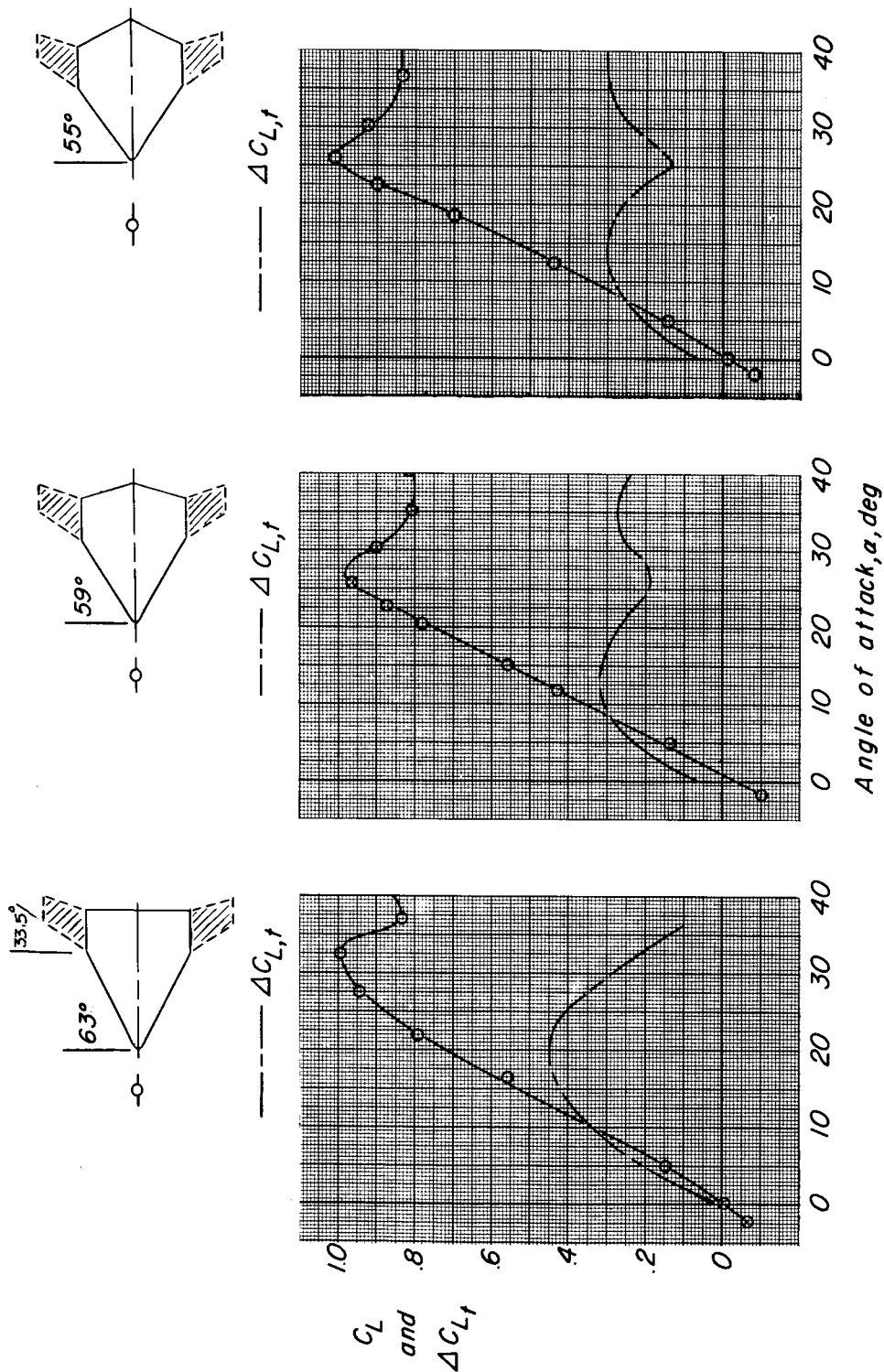


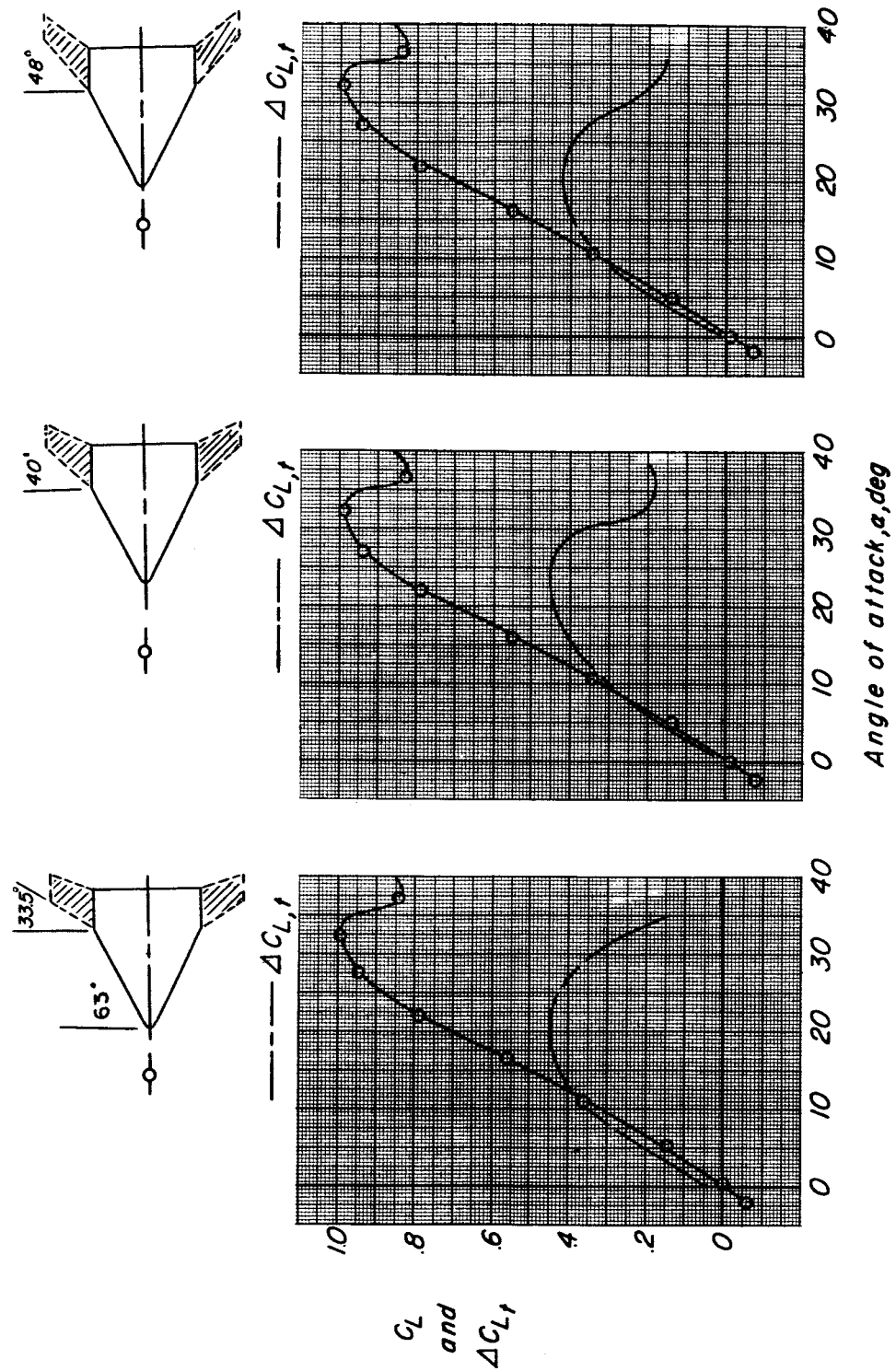
Figure 9.- The effects of wing-tip-panel dihedral angle on the variation of aerodynamic characteristics with angle of attack for the 550 and 630 sweptback wings simulating reentry, transposition, and glide-flight conditions. $St/S_w = 0.32$.



(a) The effects of wing leading-edge sweep. Vertical tails on; $St/St_w = 0.32$.

Figure 10.- Configuration effects on the lift provided by the addition of the wing-tip panels in comparison with the wing-fuselage lift at a Mach number of 0.60.

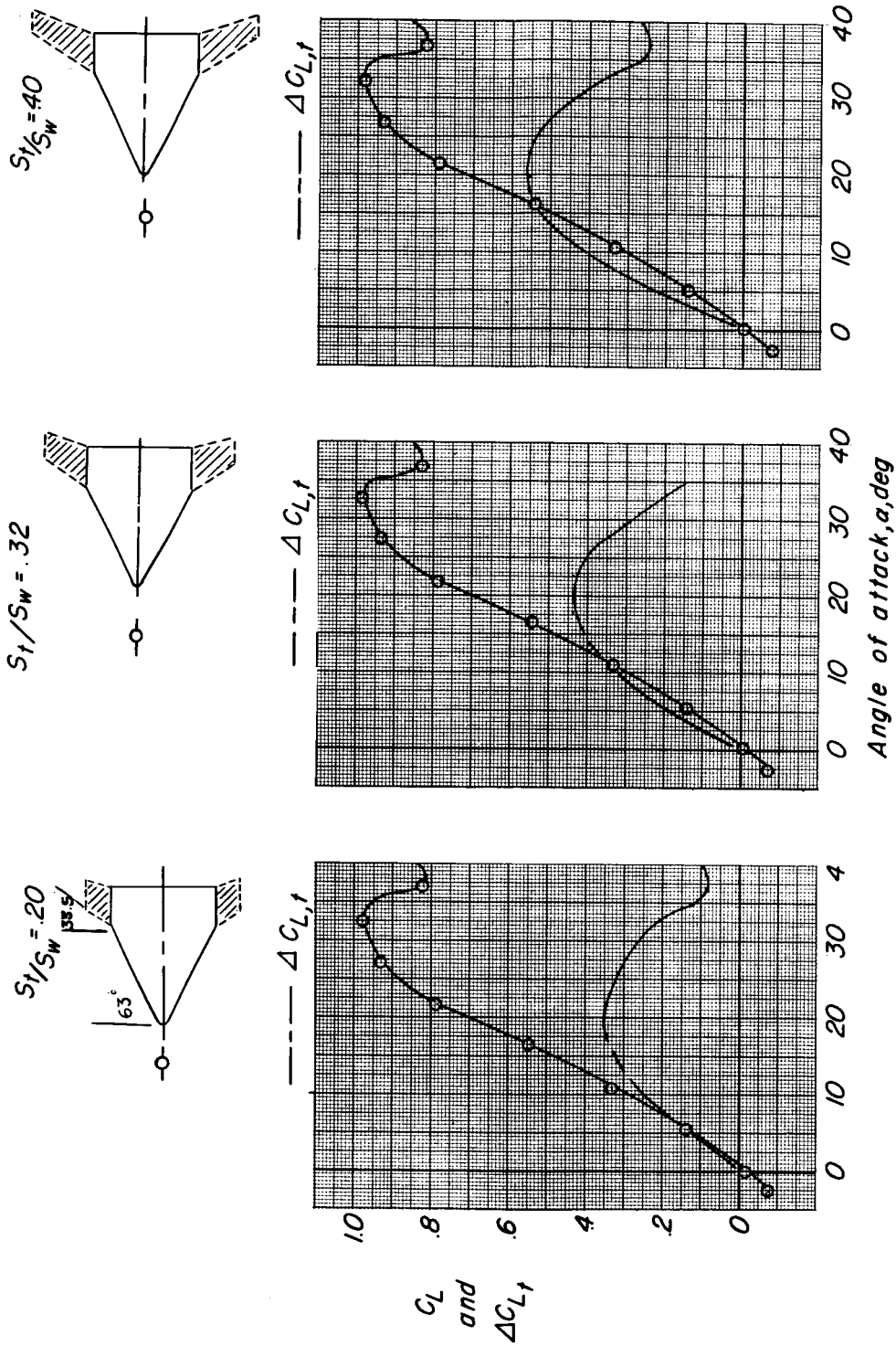
DECLASSIFIED



(b) The effects of wing-tip-panel sweep. Vertical tails on; $St/S_W = 0.32$.

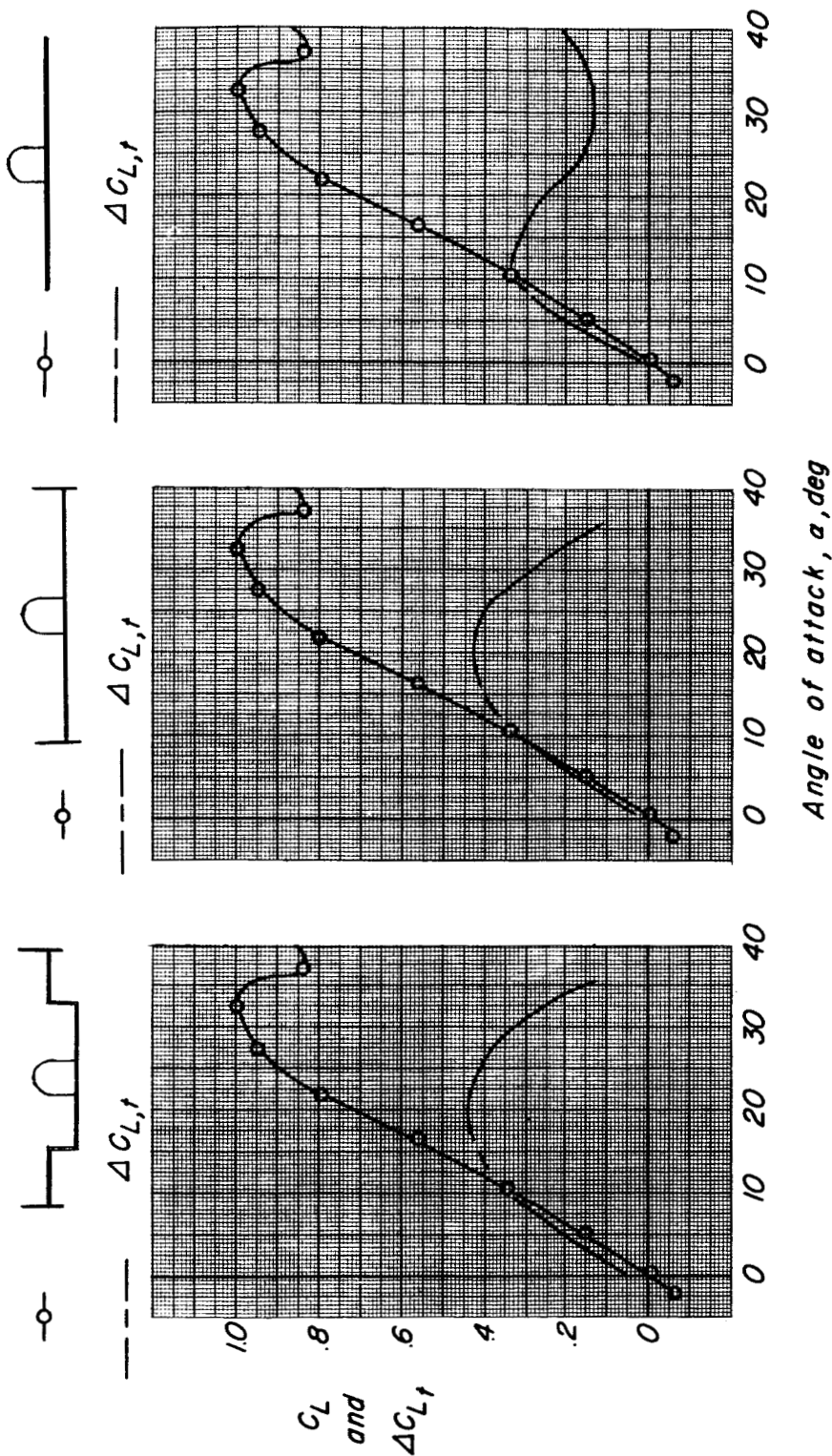
Figure 10.- Continued.

03175-1030



(c) The effects of horizontal-tail size. Vertical tails off.

Figure 10.- Continued.



(d) The effects of vertical tail and wing-tip-panel displacement for the configuration having a 63° sweptback wing. $\Lambda_{te,t} = 33.5^\circ$; $St/S_W = 0.32$.

Figure 10.- Concluded.